Holographic inscription of helical wavefronts in a liquid crystal polarization grating

Hyunhee Choi, J. H. Woo, and J. W. WuDong-Wook Kim and Tong-Kun LimSeok Ho Song

Citation: Appl. Phys. Lett. **91**, 141112 (2007); doi: 10.1063/1.2793173
View online: http://dx.doi.org/10.1063/1.2793173
View Table of Contents: http://aip.scitation.org/toc/apl/91/14
Published by the American Institute of Physics

Holographic inscription of helical wavefronts in a liquid crystal polarization grating

Hyunhee Choi, J. H. Woo, and J. W. Wu[a)]
Department of Physics and Division of Nano Sciences,Ewha Womans University, Seoul 120-750, Korea

Dong-Wook Kim and Tong-Kun Lim
Department of Physics, Korea University, Seoul 136-713, Korea

Seok Ho Song
Department of Physics, Hanyang University, Seoul 133-791, Korea

(Received 27 June 2007; accepted 11 September 2007; published online 3 October 2007)

A space-varying polarization hologram (PH) grating is fabricated in a nematic liquid crystal (LC) cell with azo-side-chain polymer alignment layers. The polarization-sensitive photoisomerization property of azo-side-chain polymer is utilized to inscribe the PH in a LC cell. Both transmission and reflection holographic configurations are adopted in fabrication. The transmission PH made by the circular orthogonal polarizations exhibits the polarization-controlled Laguerre-Gaussian beam generation, while the reflection PH made by the linear orthogonal polarizations generates a variety of Laguerre-Gaussian beam, though not polarization controlled. © *2007 American Institute of Physics*. [DOI: 10.1063/1.2793173]

Photon possesses orbital angular momentum (OAM) as well as spin angular momentum,[1] and it has been pointed out that the photon's OAM is another degree of freedom in preparing a quantum state of light for quantum optics.[2–4] To generate Laguerre-Gaussian (LG) beams possessing OAM from a planar wavefront beam, various means have been employed including a mode converter by a set of cylindrical lens, a spiral phase plate, and a computer generated hologram (CGH). In all the above examples, however, the polarization state of the LG helical wavefront remains the same as that of the incident beam.

If control of the OAM state by the input polarization is facilitated in the LG beam generator, a versatility is provided in preparing the OAM state, enabling a wide open design capability for photonic circuit incorporating multistate information encoding in quantum communication.[5] For example, it is possible to switch among different OAM's by a fast electro-optic control of the input polarization. Related to this, a nematic planar liquid crystal (LC) *q*-plate structure has been demonstrated as a polarization controlled LG beam generator, providing LG_0^2 helical modes.[6–8]

On the other hand, polarization grating is an optical element where the incident beam undergoes a polarization change upon diffraction. In the holographic fabrication of a polarization grating, two orthogonally polarized beams interfere inside a polarization-sensitive recording medium, imprinting a replica of the polarization interference pattern as a polarization hologram (PH).[9,10] If a helical wavefront beam is made to interfere with a planar wavefront reference in an orthogonal polarization configuration, the resulting PH grating possesses a space-varying polarization modulation and works as a polarization controlled LG beam generator.

In this letter, we report on the fabrication of a space-varying polarization hologram (SVPH) grating in a nematic LC cell with azo-side-chain polymer alignment layers. The polarization-sensitive photoisomerization property of azo-side-chain polymer is utilized to inscribe the PH in a LC cell. The polarization modulation gives rise to a PH in the LC cell through the photoisomerization of azo moieties on the photoalignment layer surface. Both transmission and reflection holographic configurations are adopted in fabrication. The diffraction order from the PH grating is characterized to find whether the LG beam generation can be controlled by the input polarization. The transmission PH made by the circular orthogonal polarizations exhibits the polarization-controlled LG beam generation, while the reflection PH made by the linear orthogonal polarizations generates a variety of LG beam, though not polarization controlled.

In order to inscribe the PH grating inside a birefringent nematic LC cell, we fabricated a nematic LC cell with azo-side-chain polymer alignment layers, following the procedure detailed in Ref. 11. Two beams in orthogonal polarizations from the 514.5 nm line of an Ar^+ laser are adopted as writing beams. The intensity of writing beams is 200 mW/cm^2 and the exposure time is 30 s. CGHs are used to obtain helical wavefronts to inscribe a SVPH, which was stable at room temperature and ambient light environment.

First, we adopted a transmission holographic configuration with two beams in left-/right-circular orthogonal polarizations. The 0 order and +1 order from the LG_0^2 CGH co-propagate with a small intersecting angle, providing the interference of planar wavefront (LG_0^0) and helical wavefront (LG_0^2) with the electric field of the linear polarization going through a circular rotation.[9,10] Once the SVPH grating is fabricated, we set up a Mach-Zehnder interferometer (MZI) using the light source of 632.8 nm He–Ne laser, in order to identify the detailed phase front shape of the diffracted orders. Figures 1(a) and 1(c) [Figs. 1(b) and 1(d)] show the +1 (−1) diffraction order for a right- (left-)circularly polarized planar wavefront. We find that there appears only positive or negative mode helical wavefront diffraction order with the sense of circular polarization reversed. That is, the helical mode of diffraction order LG beam depends on the polarization state of reference planar wavefront. Space-varying po-

a)Electronic mail: jwwu@ewha.ac.kr

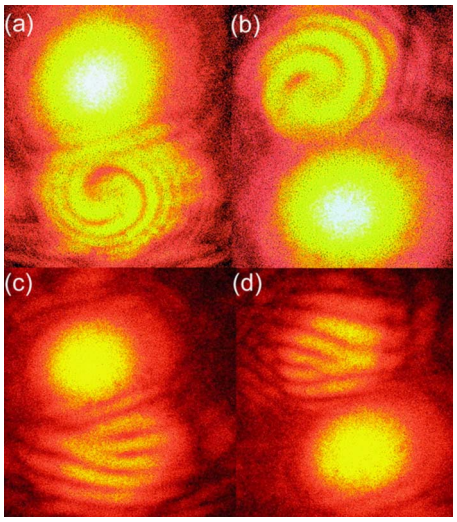

FIG. 1. (Color online) (a) and (c) [(b) and (d)] show the +1 (−1) diffraction order for the right- (left-)circularly polarized planar wavefront.

larization state manipulation has been demonstrated in a midinfrared wavelength by use of the subwavelength grating technology because of the difficulty in mechanical fabrication of a polarization grating with the period comparable to the optical wavelength.[12] Our SVPH grating, fabricated by a transmission holographic configuration, allows the desired space-varying polarization state manipulation in the range of the visible wavelength. Although it is straightforward to fabricate LG beam generator with helical modes other than LG_0^2, our example shows that the *q*-plate structure can be readily attained by a SVPH grating fabrication.

Next, in order to further investigate the versatility of the PH in generating helical wavefronts, we extended our study to a reflection holographic configuration. Refer to the reflection holographic configuration shown in Fig. 2. We inscribed three PHs by superimposing different diffraction orders generated from the LG_0^1 CGH, that is, the 0 and ±1 orders. The three PHs are (a) the interference of two +1 orders of helical wavefronts (LG_0^1), (b) the interference of 0 order planar wavefront (LG_0^0) and +1 order of helical wavefront (LG_0^1), and (c) the interferencem of +1 and −1 orders of helical wavefronts (LG_0^1 and LG_0^{-1}). In each case, the resulting

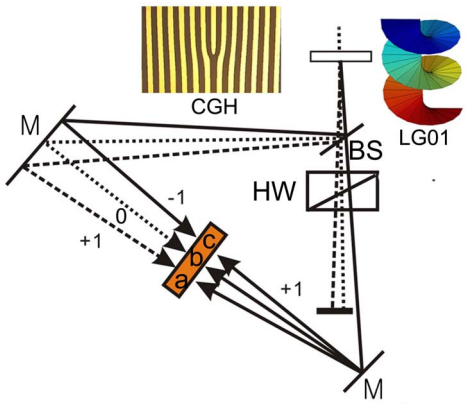

FIG. 2. (Color online) The slanted reflection holographic configuration to inscribe the *S*- and *P*-polarization modulations. (a)–(c) in the PH LC grating correspond to the recording condition for Figs. 3(a)–3(c), respectively. (CGH: computer generated hologram of LG_0^1 mode, BS: beam splitter, HW: half-wave plate, and M: Mirror.)

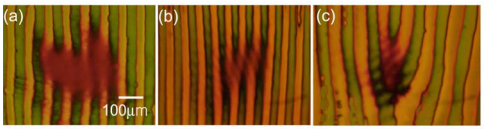

FIG. 3. (Color online) The microscopic texture of PHs (a) LG_0^1 and LG_0^1, (b) LG_0^1 and LG_0^0, and (c) LG_0^1 and LG_0^{-1} mode writing beams, counterpropagating in linear orthogonal *S*/*P* polarizations.

space-varying phase difference $\phi(x,y)$ is (a) zero, (b) $\tan^{-1}(y/x)$, and (c) $2\tan^{-1}(y/x)$. Once the PH is inscribed into the LC cell, the LC polarization domains inside the PH grating were examined by a polarized microscopy. Figures 3(a)–3(c) are the textures of LC domains of three PHs observed in the polarized microscopy, corresponding to the PHs (a)–(c). In the PH (a), the phase difference is independent of *y*, resulting in a linear polarization grating with the grating vector along *x* axis, as seen in Fig. 3(a). Note that there exists a central blurred spot where no polarization grating pattern is present, which results from the fact that both writing helical wavefronts have zero light intensity at the center of beams profile due to the phase singularity of a helical mode, and no photoisomerization process takes place in the region of the zero light intensity of two superimposed beams, hence no rotations of LC molecules. In Fig. 3(b), corresponding to the PH (b), LC polarization domains have a pattern of a two-pronged fork grating in the polarized microscopy texture. Figure 3(c), corresponding to the PH (c), shows three-pronged fork grating patterned LC polarization domains. Here, similar to the patterns in Fig. 3(a) a central disk of zero light intensity formed by two superimposed helical modes leaves the LC molecules within the disk unrotated, which results in the breaking of the central prong at the branching point of the three-pronged fork.

The observed LC polarization domain structure of the space-varying polarization LC grating can be understood from a theoretical simulation of the polarization modulation on the hologram surface. Figure 4(a) is the simulation result of the interference modulation formed by a helical wavefront LG_0^1 and a planar wavefront LG_0^0 beams. The left part of Fig. 4(a) is colored for ease of illustration of the polarization grating shape. The red and blue domains are adjacent to each other, the LC directors of two domains are oriented in opposite angles with respect to the *y* axis, and the spatial distribution of two domains has one dislocation on the *y* axis, which is the fork grating. Figure 4(b) is the enlarged figure of the rectangular area of Fig. 4(a), showing the detailed peri-

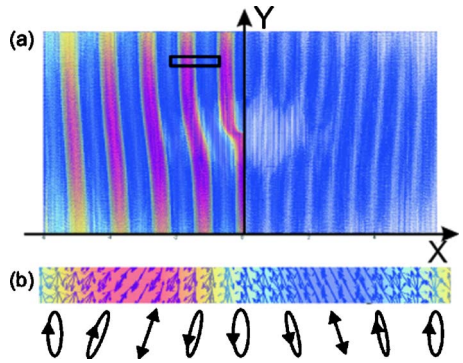

FIG. 4. (Color online) Simulation of PH grating, shown in Fig. 3(b). (b) The enlarged image of rectangular part of (a) with the polarization modulations of a reverse twisted LC domain.

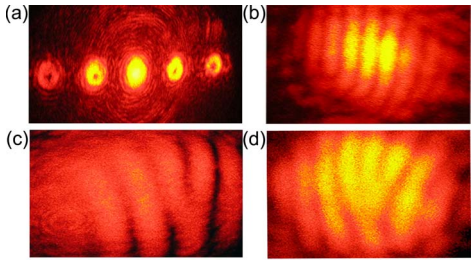

FIG. 5. (Color online) Diffraction orders from PH shown in Fig. 3(b). (b)–(d) are the interference patterns of +1 order from PH in Figs. 3(a)–3(c) with a planar wavefront reference, respectively.

odic polarization modulation change due to the phase differences. Differently from the transmission hologram, the reflection hologram gives rise to the LC polarization grating in the structure of reverse twisted nematics (RTNs), which we call the space-varying RTN polarization grating.[11]

In order to understand how the polarization state will change upon diffraction from the space-varying RTN polarization grating, the Jones matrix should be derived, which can be done by taking into account the spatial distribution of two TN domains with opposite sense of rotation. Aside from the optical phase term coming from the space-varying phase difference, the resultant Jones matrix takes the following form:

$$\mathbf{M}^0 = \begin{pmatrix} a+b & 0 \\ 0 & a-b \end{pmatrix},$$

$$\mathbf{M}^{\pm 1} = \pm \begin{pmatrix} 0 & c-d \\ c+d & 0 \end{pmatrix}, \tag{1}$$

where $a-d$ are complex numbers determined by the geometric dimensions of the grating such as birefringence n_e-n_o, cell thickness, the tilt angle, and the off-set angle of TN inside the grating. We note that Jones matrix forms of the 0 and ±1 orders are different. When the incident beam is *S*-or *P*-linearly polarized, the ±1 diffraction orders get the polarization changed, while the 0 order keeps the polarization unchanged. For a left-or right-circular polarized beam, both 0 and ±1 diffraction orders are in an elliptical polarization, the ellipticity being determined by the ratios a/b and d/c.

Now, we investigate the diffraction characteristics of the space-varying RTN polarization grating by irradiating with the *S*-linearly polarized probe beam of 632.8 nm He–Ne laser. As shown in Fig. 5(a), the ±1 diffraction orders have annular intensity distributions and the polarization was measured to be 90° rotated, while the 0 diffraction order has a Gaussian intensity distribution with the polarization state unchanged. In order to identify the detailed phase front shape of diffracted orders from the RTN polarization grating, we set up a MZI again. There occurs an intensity modulation with the intensity fringe patterns, as shown in Figs. 5(b)–5(d) each corresponding to the PH in Figs. 3(a)–3(c), respectively. We clearly observe a linear, a two-pronged fork, and a three-prong fork shaped fringe patterns.

When a right- (left-)circularly polarized planar wavefront beam is incident on the grating, the intensity fringe patterns were observed to be the same as those in Fig. 3, while the polarizations of both 0 and ±1 diffraction orders are measured to be linearly polarized with the polarization direction making an angle of −45° (+45°) relative to the *y* axis. We estimated the experimental values of the tilt angle and the off-set angle and obtained the ratio of ≈1 for both a/b and d/c, which corresponds to a linear polarization according to Eq. (1).

In summary, we fabricated a space-varying polarization hologram grating in a LC cell. Depending on the configuration of two orthogonal polarizations of writing beams, a variety of polarization control of LG beam generation can be achieved. In the transmission hologram, the helical mode of the diffraction order can be controlled by the input polarization of a planar wavefront. In the transmission hologram, the reverse twisted nematic polarization grating was fabricated, which generates LG helical wavefront possessing an orbital angular momentum.

J.W.W. acknowledges the support by Seoul Research and Business Development Program (10816), by ABRL program, and by Korea Research Foundations (KRF-2006-005-J04001), and S.H.S. acknowledges the support by OPERA ERC program.

[1] L. Allen, S. M. Barnett, and M. J. Padgett, *Optical Angular Momentum* (Institute of Physics, Bristol, 2003).
[2] A. Mair, A. Vaziri, G. Weihs, and A. Zeilinger, Nature (London) **412**, 313 (2001).
[3] J. Leach, M. J. Padgett, S. M. Barnett, S. Franke-Arnold, and J. Courtial, Phys. Rev. Lett. **88**, 257901 (2002).
[4] A. Vaziri, G. Weihs, and A. Zeilinger, Phys. Rev. Lett. **89**, 240401 (2002).
[5] G. Gibson, J. Courtial, M. J. Padgett, M. Vasnetsov, V. Pas'ko, S. Barnett, and S. Franke-Arnold, Opt. Express **12**, 5448 (2004).
[6] L. Marrucci, C. Manzo, and D. Paparo, Appl. Phys. Lett. **88**, 221102 (2006).
[7] L. Marrucci, C. Manzo, and D. Paparo, Phys. Rev. Lett. **96**, 163905 (2006).
[8] D. Voloschenko and O. D. Lavrentovich, Opt. Lett. **25**, 317 (2000).
[9] H. Ono, A. Emoto, F. Takahashi, N. Kawatsukib, and T. Hasegawa, J. Appl. Phys. **94**, 1298 (2003).
[10] L. Nikolova and T. Todorov, Opt. Acta **31**, 579 (1984).
[11] H. Choi, H. J. Chang, B. Park, and J. W. Wu, Appl. Phys. Lett. **88**, 021905 (2006).
[12] Z. Bomzon, G. Biener, V. Kleiner, and E. Hasman, Opt. Lett. **27**, 1141 (2002).